

JAROSŁAW BARTOSZEWICZ\*

Poznan University of Technology  
Chair of Thermal Engineering  
Poznań

## Analysis of heat load in a biomass-fired boiler

This paper discusses an exemplary cooperation between a research center, industry and technical inspection authorities. The purpose of the investigations (carried out to find the failure of a biomass-fired boiler in a heating plant) is an analysis of the effect of operating water boiler conditions on the heat load of the heating surface. The analysis concerns the reasons for failure of the membrane heat exchanger of the water-gas type being a basic heating surface of the boiler burning biomass. During the operation of the boiler some cracks perforated the bottom and smoke tube endings occurred.

### 1 Introduction

In the age of an intense development of the numerical techniques there is a new possibility of using more and more advanced software for mass flow, momentum and energy analysis. At the moment there are several computer programs available in the market that enable getting satisfactory results of the flow analysis in heat and flow machines. Unfortunately, a great complexity of codes and most often a significant complexity of the analyzed problems considerably limit the accessibility to those sources of information. Despite such limits there are many research centers equipped with computer programs and providing sufficient technical expertise whose software applications can be used. In a power station of Trzcianka two high temperature water boilers were installed, both about 5 MW. The boilers fitted with an economizer were heated with biomass in the form of woodchips. Both boilers were considered as basic units that were used for heating the water supplying the town heat distribution network. The subject of the analysis was a heat exchanger that considered a heat receiver in both boilers. Based on the boiler manufacturer specifications the minimum flow of water was 42 m<sup>3</sup>/h (0.01166 m<sup>3</sup>/s) and the maximum flow of water was 180 m<sup>3</sup>/h (0.05 m<sup>3</sup>/s) at the realized operating medium temperature increment  $\Delta T = 25$  K. The boiler

---

\*E-mail: jaroslaw.bartoszewicz@put.poznan.pl

units were automatically operated. The automatics controlled the supply and the combustion of fuel (air and exhaust gas fans, hydraulic push rod, fire flap) and maintained the required temperature of water at the boiler outlet (required temperature difference of  $\Delta T = 25$  K and the minimum return temperature 343 K). The hydraulic exhaust gas flow circuit for boilers and the heat distribution network were not fitted with the hydraulic push rod. Instead pumps were fitted, which resulted in significant changes in the boiler pressure values as it could be concluded from the analysis of the recorded bar charts.

## 2 The object of analysis

The schematics of a water boiler, which was heated with woodchips and fitted with a steel membrane heat exchanger, has been presented in Fig. 1. The boiler consisted of a ceramic combustion chamber and a mechanical stoker cooled with water (1), ceramic exhaust gas manifolds (2, 3), a membrane heat exchanger of exhaust gas-water type consisting of a return chamber (4) directing the exhaust gas flow towards the first bank of smoke tubes (8), a back return chamber (5), the second bank of smoke tubes (9), a collecting chamber with a flue and a heat exchanger (7) protecting the boiler against an excessive temperature increase. In order to ensure complete fuel combustion possible the boiler was made of chamotte brick.

A proper exhaust extended manifold that shaped the way has been used thereby providing some extension of the burning time of volatile matter. The specified nominal boiler parameters were as follows: operating pressure 1 MPa, heating power 5 MW, max. outlet water temperature 403 K, min. inlet water temperature 343 K, exhaust gas temperature 493 K, boiler heating surface area 390 m<sup>2</sup>, water capacity 9.5 m<sup>3</sup> and thermal efficiency 85%.

The schematics of the bottom part of the steel heat exchanger (exhaust gas-water type) have been shown in Fig. 2. The heat exchanger consisted of two perforated bottoms of 1.970 m in diameter, between which there were four bundles of pipes with dimensions of  $D = 60 \times 3.2$  mm and length of 5 m. The two lower bundles formed the first exhaust gas draught of the heat exchanger closed by a return chamber and two upper bundles from the second exhaust gas draught closed by a collecting chamber with the flue.

Exhaust gases from the biomass combustion process flowed out through a rectangular ceramic pipe and while in the return chamber (item no. 4 in Fig. 1) they changed their direction of flow into horizontal. In this chamber, made from profiled elements cooled with water, after changing the flow direction the ex-

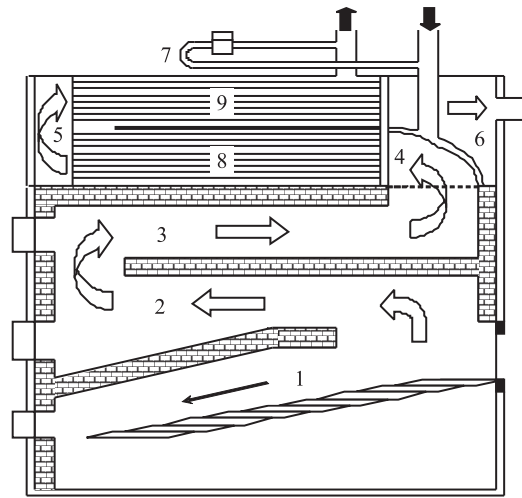


Figure 1. The schematics of water biomass-fired boiler.

haust gases from the back of the return chamber flowed through the two upper bundles of pipes. The water was supplied to the heat exchanger from an arc-collecting manifold. Some water was transported throughout six rectangular openings ( $175 \times 50$  mm – 2 inlets,  $200 \times 50$  mm – 4 inlets) symmetrically arranged along the horizontal axis of the perforated bottom and flowed into the exchanger under a plate that separates the upper section of the pipe bundles from the lower one. Water was supplied from the lower part of the manifold through five openings  $D = 0.08$  m arranged on the arc of the heat exchanger shell perpendicularly to the pipes, as marked with black arrows in Fig. 2.

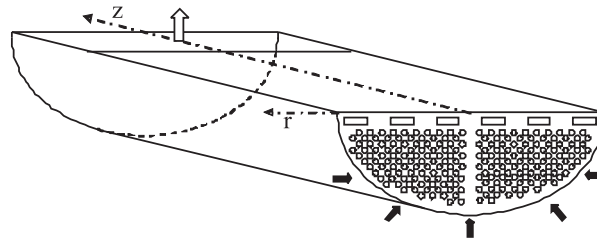


Figure 2. The model of pipe banks in the first draught of the heat exchanger.

The perforated bottoms and smoke tubes of the exchanger were made of steel specified in Tab. 1. The first perforated bottom and the smoke tube endings were exposed to the highest thermal loads, which reduced the strength of steel. The strength of the St 41-K steel decreased as a function of temperature [4], as shown in Tab. 2.

Table 1. The construction materials.

Heat exchanger	Material	Dimensions [mm]
Perforated bottom	St 41-K	12
Smoke tube	St 35.8	60.3×3.2

Table 2. The acceptable limits of plasticity of steel St 41-K.

$T$ [K]	293	473	523	573	623	673	723
Re [MPa]	260	210	190	160	140	120	100

From one side the first perforated bottom of the heat exchanger was exposed to a high temperature exhaust gas flowing with the temperature exceeding 973 K. The other side of the perforated bottom was in contact with water at a minimum temperature of 343 K. On the perforated bottom occur two effects. The first one is growth of temperature strength in steel, and the second one is pulsation of pressure from three mixing pumps. The higher the temperature of the heat exchanger perforated bottom, the greater stresses were observed. The accurate determination of the steel strength reduction extent is difficult to perform because of the complexity of effects involved and some irregularity in the heat loads. When analyzing the reference data [1] we should note that the materials used for the construction of the heat exchanger meet the requirements of the relevant standards and they should not be a reason for the failure in a typical boiler operation.

### 3 The numerical analysis

The numerical calculations were performed with the use of the Phoenics software. The numerical method used to carry out the calculations was presented in the

paper [6]. The software provides solutions to the discretized versions of sets of differential equations having the general form of:

$$\frac{d(\rho\varphi)}{dt} + \text{div}[\rho\mathbf{u}\varphi - G \text{grad}(\varphi)] = S, \quad (1)$$

where  $\rho$  stands for density,  $\varphi$  stands for any conserved property (such as temperature, enthalpy, momentum per unit mass, mass fraction of chemical species, turbulence energy, etc.),  $\mathbf{u}$  stands for the velocity vector,  $G$  and  $S$  stand for the exchange coefficient of the entity  $\varphi$  and the source rate of  $\varphi$ . Moreover, the numerically solved system of equations includes a system of complementary equations presenting a model of turbulence. In the performed analyses a model of turbulence  $k$ - $\varepsilon$  for small Reynolds numbers was used as proposed by Lam and Bremhorst [2]. This model is one of the simplest modifications of a standard model  $k$ - $\varepsilon$  for high Reynolds numbers [3] allowing its use in the case of flows that are characterized by a low turbulence, as it was observed for the discussed flow. The assumed model allows indirect determining of two parameters describing the turbulence in the kinetic turbulence energy flow and a rate of the turbulence energy dissipation.

The schematics of the discussed boiler with a heat exchanger have been shown in Fig. 1. In parts marked 2 through 6 it was loaded to the Phoenics computer software as a geometry to be analyzed in order to solve the problem of exhaust gas and water flows as well as to determine the effect of water and gas flows on the heat exchange characteristics within the first perforated plate. The numerical calculations were analyzed in two steps. The first step analysis concerned the exhaust gas flow within the last draught of the boiler and the first draught of the heat exchanger in order to check the uniformity of the exhaust gas distribution in the lower pipe bundles of the heat exchanger and to determine the effect of the flow separations occurring at the flow edges in the profiled return chamber. The second step analysis contained an evaluation of the water flow inside of the heat exchanger within its first draught.

## 4 Results and discussion

The presentation of the results concerning the exhaust gas is limited to the last ceramic draught and the first draught of the heat exchanger. A distribution of velocities in the considered fragment has been shown in Fig. 3. The presented figures indicate some diversification of the exhaust gas velocity values caused by different shapes of the exhaust gas manifolds and their sizes.

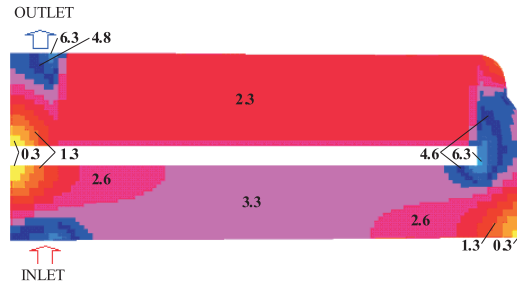


Figure 3. The distribution of velocity, [m/s].

The exhaust gases flowed in the last ceramic draught of the boiler through the rectangular opening. Then, the exhaust gases changed their direction into horizontal according to the manifold arrangement. The exhaust gases flowing into the heat exchanger flow in a two-arc manifold properly shaped enabling a uniform exhaust gas distribution among the first draught smoke tubes of the heat exchanger. As it can be seen in the relevant drawings there is a correct distribution of the mass flows because a mass flow is a linear velocity function. Figure 3 shows that there was no significant velocity change along the perforated bottom height which denotes a non-uniform flow of the exhaust gases in the first bank of the smoke tubes.

The next parameter which was analyzed in the numerical calculations was the exhaust gas temperature decrease during the flow in the heat exchanger pipes. A distribution of the exhaust gas temperature change during its flow through the manifold of the last ceramic boiler draught and the first heat exchanger draught has been presented in Fig. 4. After analyzing the distribution of the exhaust gas temperature and comparing it with the velocity distributions a uniformity of dis-

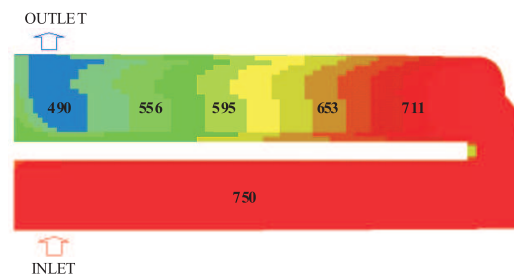


Figure 4. The distribution of temperature, [°C].

tributions in the cross-sections of the exhaust gas manifolds has been seen. There was a significant decrease in the exhaust gas temperature along the way of the exhaust gas flow through the heat exchanger, resulting from the heat exchange between the hot exhaust gas flowing inside and water outside the piping. These changes were small across the exchanger. There were no significant temperature changes in the ceramic part.

The distribution of the exhaust gases kinetic energy of turbulence changes caused by their flow through a profiled return chamber and their inflow onto the exchanger-perforated bottom has been shown in Fig. 5. The obtained results show that at points where the main direction of flow changed, some flow separations were formed on the constructional surfaces as well as a wake formed by the flowing-off swirls. This complex swirl structure has two characteristic features: it makes the exhaust gas flow across the wake difficult and significantly increases the heat transfer coefficient at the perforated bottom. The wake moved along the whole perforated bottom of the first bank of pipes. Consequently, the exhaust gas flow blockage was uniform along the whole height and did not cause any significant changes in the distribution of mass flowing through individual smoke tubes. The second effect of the wake was more important from the point of view of the failure analysis. The exhaust gas flow of high turbulence moved along the perforated bottom and intensified the heat exchange between the perforated bottom surface and exhaust gases.

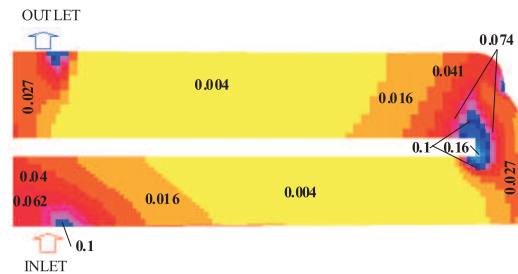


Figure 5. The distribution of kinetic energy of turbulence,  $[\text{m}^2/\text{s}^2]$ .

The performed numerical calculations show that the exhaust gas flow was uniformly distributed inside the pipe bundles however, at the same time the perforated bottom surface had to carry significantly higher heat loads caused by an increase in the heat transfer coefficient due to the increased intensification of gas turbulence. This means that an increased receipt of heat flow from the exhaust gases should be guaranteed on the waterside.

The next step of the investigations dealt with an analysis of the water flow inside the heat exchanger and included the determining of the velocity distributions. The structure of a flow inside the jacketed exchanger is very complex. It is determined by the location of the input openings and an arrangement of pipes in the individual bundles in relation to the direction of the water outflow. In order to explain the mass transport mechanisms three control sections were used. The location of the control sections has been shown in Fig. 6. Two control sections were located in the transverse plane in the distance of 50 mm and 500 mm from the perforated bottom, respectively, and one in the longitudinal plane in a distance of 500 mm from the axis of the heat exchanger. The redistributions of the velocity in sections were normalized by the local maximum velocity.

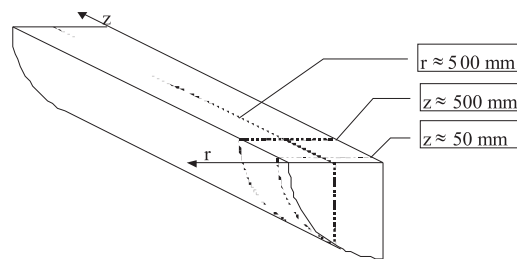


Figure 6. The principal section in first part of heat exchanger.

The distributions of velocity in the transverse plane showing its changes in the vicinity of the first perforated plate are presented in Figs. 7 and 8. The obtained data show that a stream flowing out from the openings located in the central part of the perforated bottom, under the plate separating the draughts of flows of the heat exchanger along the pipes, only slightly propagated in a radial direction. The openings arranged circumferentially were to provide cooling smoke tubes with water.

However, numerical calculations show that, due to the pipes packed too close, water cannot be fed to some areas of the heat exchanger and its direction of flow quickly changes into the axial one. The problem with the heat exchanger appears in situation, when axial and radial components of velocity are equal to zero. The white areas corresponding to the minimum or zero velocity of flow between the smoke tubes would not exist. The analogical solutions for the distance of 0.5 m from the perforated bottom have been shown in Fig. 8. The axial component indicates a gradual but very slow propagation of flows in a radial direction. The distribution of the radial component presented in Fig. 8b shows that at the distance of 0.5 m from the perforated bottom the maximum velocity



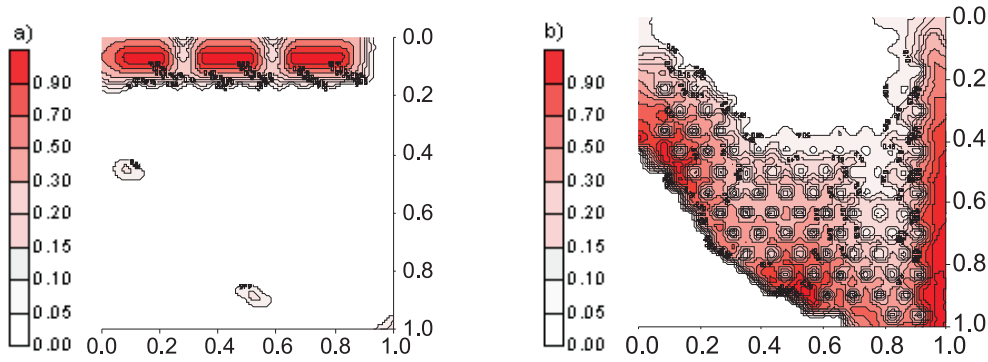


Figure 7. The normalized distributions of axial component (a) and radial component (b) of velocity in section  $z = 50$  mm.

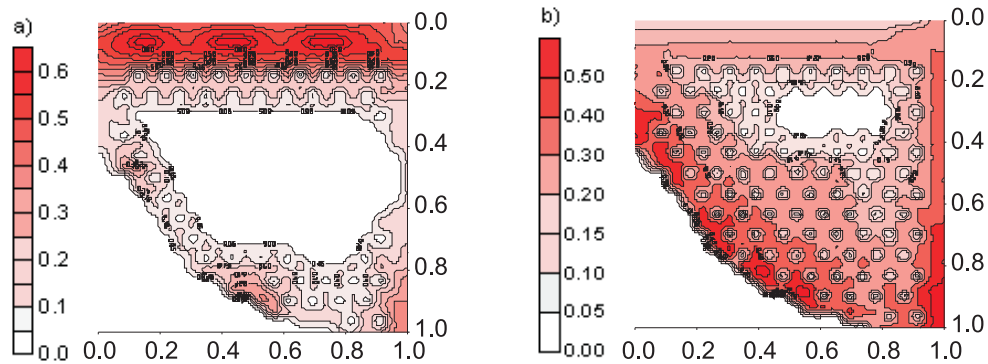


Figure 8. The normalized distributions of axial component (a) and radial component (b) of velocity in section  $z = 500$  mm.

area fades. A lack of the mass exchange, anywhere inside the heat exchanger may mean an occurrence of local overheating or even boiling water states.

The axial and radial velocity components in the longitudinal plane distant of 500 mm from the exchanger axis have been shown in Fig. 9. The superimposed white areas in Figs. 9a and 9b show that there was a small area of a very small mass exchange close to the perforated bottom. A thermal power taken away from the perforated bottom surface and pipes was a mass function being a velocity function. Small velocities correspond to a decrease in the mass flow acting on the perforated bottom surfaces which at a constant heat flow supplied from the exhaust gas side, results in an increase in the wall temperature and, subsequently, an increase in the water temperature. The results of the numerical

calculations prove the occurrence of two superimposing effects. First, a flow of heat transferred from the exhaust gases to the wall was greater due to an increase in the turbulence of flow caused by a wake formed in the exhaust gas return area. This resulted in an increase in temperature of the perforated bottom. Second, a disturbed water flow at the perforated bottom area in the central part of the bundle resulted in a smaller heat receipt and caused an even more intensive increase in the wall temperature. Analyzing the failure causes, the technical inspection revealed the effects of such a phenomenon confirming the above hypothesis. During the visual inspection of the boiler, some boiler scale deposit was found on the surface of the perforated bottom and on the pipes at their contact with the perforated bottom. This unquestionable proof seems to verify the results of the numerical calculations, as the boiler scale deposits only in the overheating water areas or in the phase transition areas. The statement that a disturbed water flow in a certain part of the heat exchanger caused a sudden increase in water temperature (resulting in the boiler scale deposition) seems to be right. Next, the growing boiler scale layer reduced additionally the receipt of the wall heat by water, thus leading to an even greater increase in the wall temperature.

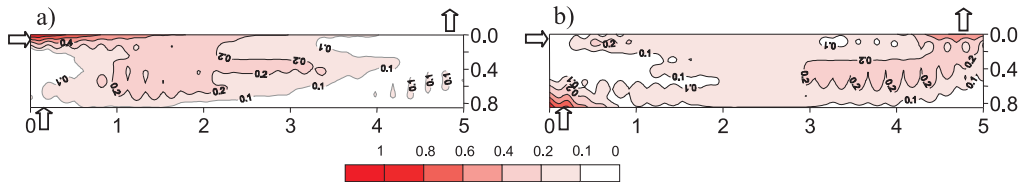


Figure 9. The normalized distributions of axial component (a) and radial component (b) of velocity in section  $r = 500$  mm.

The heat exchanger failure was caused by numerous cracks of the smoke tubes at their connections with the exchanger draught perforated bottom. The cracks that were propagating in the pipe joined the perforated wall and propagated in the wall material. The relevant photos presented in Fig. 10 show the places where the cracks of the smoke tubes and the perforated bottom material occurred. The cause of failure can be determined based on those photos and information on the boiler operating conditions, which, in general, may concern many factors responsible for the failure acting at that time. Among them, an effect of the high temperature exhaust gas flow on the perforated wall combined with the periodic pressure changes caused by the automatics controlling the pump mixing units, and a lack of the mass change on the water side should be mentioned. The point

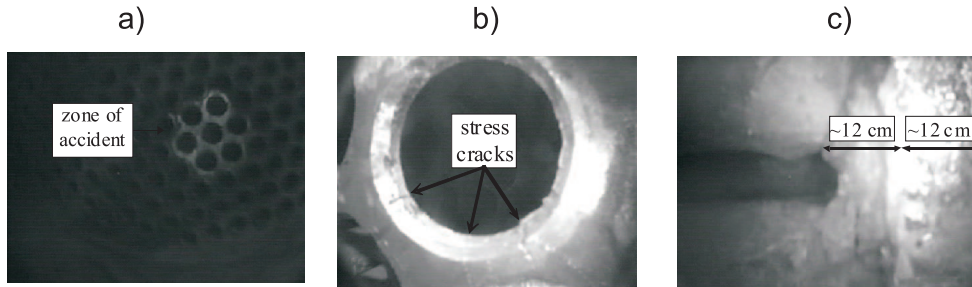


Figure 10. Small break loss of coolant accident (a), stress crack of smoke tube and perforated bottom (b) thickness of boiler scale and perforated bottom (c).

of attachment of the smoke tube and perforated bottom is the weakest link in all heat exchanger.

The deposit thickness was of 5 to 15 mm. The analysis of a water sample taken from the heating system showed that the total water hardness of  $0.065 \text{ mval/dm}^3$  was almost twice as high as the standard value  $0.035 \text{ mval/dm}^3$ . The consecutive water tests showed  $\text{pH} = 7.61$  which was too low ( $\text{pH} = 9\text{--}10$ ). The chemical analysis of the boiler scale showed the following results: the calcium compounds in the form of  $\text{CaO} - 44.0\%$ ; magnesium content in the form of  $\text{MgO} - 5.02\%$ ; carbonate content  $\text{CO}_2 - 11.4\%$ ; sulphite content  $\text{SO}_3 - 5.1\%$ ; silicate content  $\text{SiO}_2 - 7.52\%$ . The boiler scale was characterized by a small thermal conductivity in relation to steel. An additional layer on the steel increased its temperature and consequently decreased its strength.

## 5 Conclusion

The most important factors responsible for the boiler failure were determined on the basis of the multi-track analysis of data concerning the block construction, the block operation, the physical and chemical properties of water, the strength analysis of the constructional material samples taken from the heat exchanger elements and the numerical calculations carried out with the use of Phoenics software. The most probable sequence of events responsible for the failure occurrence has been presented in Fig. 11. The possible causes of the failure occurrence can be divided into four parts: quick changing oscillations of pressure caused by a lack of hydraulic coupling, improper quality of water, an increased value of the heat transfer coefficient, a stagnation area occurring in the water jacket in the vicinity of the perforated bottom.

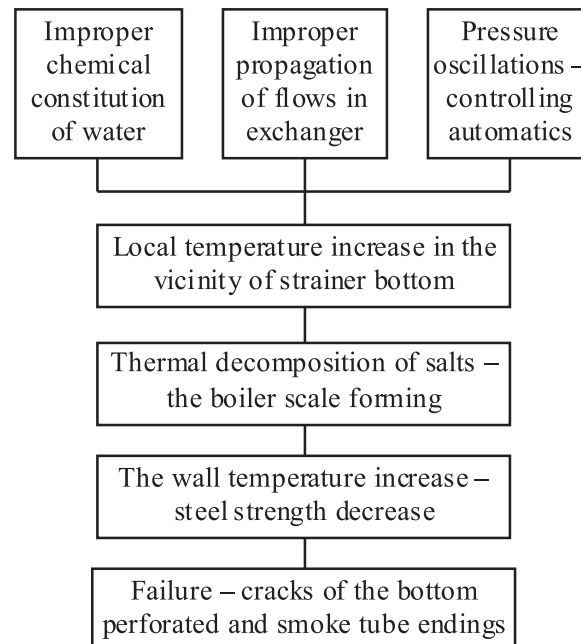


Figure 11. The reasons of water-boiler breakdown.

The reason for the failure was a decrease in the perforated bottom material strength caused by an increase in the material temperature combined with fatigue load produced by the operation of three pump mixing units and some automatic units completing the loss of water in the Trzcianka boiler plant. The considered project proved the effectiveness of the use modern computer software in the analyses of the operation of the heat and flow machines.

*Received in March 2008*

## References

- [1] Orłowski P.: *Steam Boilers. Designs and Calculations*. WNT, Warsaw 1979.
- [2] Lam C.K.G., Bremhorst K.: *A modified form of the  $k-\varepsilon$  model for predicting wall turbulence*. J. Fluids Engineering, ASME **103**, 1981, 456.
- [3] Launder B.E., Spalding D.B.: *The numerical computation of turbulent flows*. Comp. Mech. in Appl. Mech. & Eng. 3, 1974, 269.
- [4] Polish Committee of Normalization, No. PN-75/H-84024, 1975.
- [5] *Report of Examination No. 119/2005*. Office of Technical Inspection in Poland, 2005.

- [6] Rosten I., Spalding D.B.: *The PHOENICS Beginner's Guide*. CHAM Report No. TR/100, CHAM Limited, Wimbledon, England, 1985.
- [7] *Engineering Drawing of Water Boiler PR-5000*. Polytechnik Swiss AG, Bösch 37, CH-6331 Hünenberg/ZG.

### **Analiza obciążenia cieplnego w kotle opalanym biomasa**

#### **S t r e s z c z e n i e**

W artykule przedstawiono wyniki współpracy ośrodka naukowego, ciepłowni miejskiej i inspekcji technicznej realizowanych w celu wykrycia przyczyn awarii kotła opalanego biomasa. Przedstawiono wyniki analizy numerycznej oraz wizualizacji w ciepłowni w celu określenia tych przyczyn. Badania obejmowały analizę przepływu wymiennika ciepła typu woda-spaliny, który stanowi podstawową powierzchnię wymiany ciepła w kotle spalającym biomasa. Przedstawione w pracy wnioski z analizy wskazują na przyczyny pęknięć płyty sitowej i końcówek płomieniówek wymiennika.

